J Mol Model (2008) 14:489–497
DOI 10.1007/s00894-008-0297-9

ORIGINAL PAPER

Electronic properties of some nitrobenzo[*a*]pyrene isomers: a possible relationship to mutagenic activity

Vito Librando · Andrea Alparone · Gaetano Tomaselli

Received: 18 December 2007 / Accepted: 18 February 2008 / Published online: 26 April 2008

Abstract Ionization potential (IP), electron affinity (EA), dipole moment (μ) and electronic polarizability (α) of 1-, 3- and 6-nitrobenzo[*a*]pyrene isomers (1-NB*a*P, 3-NB*a*P, 6-NB*a*P) were determined by using density functional theory (DFT) and recent semiempirical PM6 methods. Calculated IP value remains almost constant along the series of isomers, while EA value depends on the nitro group position, increasing by ca. 0.2 eV on passing from 6- to 1-NB*a*P (or 3-NB*a*P) isomer. Stability, μ and α values decrease in the order 6-NB*a*P < 1-NB*a* ~ 3-NB*a*P, the largest μ variation being predicted to be 1.5 D (30%) by DFT computations. The results obtained herein are consistent with the observed greater mutagenic activity of 3- and 1-NB*a*P in comparison to 6-NB*a*P isomer, suggesting that both binding to enzyme, which depends on electric properties, and reduction process, which is related to EA value may be crucial steps in the mutagenic mechanism of this series of isomers.

Keywords Electron affinity · Electronic dipole polarizability · Dipole moment · Mutagenicity · Nitrobenzo[*a*]pyrenes

V. Librando (✉) · G. Tomaselli
Department of Chemistry, University of Catania,
Viale A. Doria 8,
I-95125 Catania, Italy
e-mail: vlibrando@unict.it

A. Alparone
Research Centre for Analysis, Monitoring and Minimization Methods of Environmental Risk and Department of Chemistry,
University of Catania,
Viale A. Doria 8,
I-95125 Catania, Italy

Introduction

Nitropolycyclic aromatic hydrocarbons (NPAHs) represent a class of genotoxic environmental contaminants usually produced from combustion processes and reactions between polycyclic aromatic hydrocarbons (PAHs) with nitrogen oxides [1, 2]. They are persistent pollutants in both gas and particulate matter phases and show considerable biological activity, often exhibiting higher mutagenic capacities than those of their parent PAHs [1–3]. In some cases they are also potent tumorigenic compounds [4]. Degradation of NPAHs is a demanding task because of their high chemical and biochemical stabilities [5]. To this purpose, specific use of naturally occurring or modified enzymes is becoming an appealing solution in bioremediation strategies of contaminated sites [5–7]. It is widely recognized that structural properties of NPAHs rule their biochemical activities. Specifically, orientation of the plane of the nitro group with respect to the plane of the aromatic system is strictly related to nitroreductive activities, capacity to bind to DNA structure and direct-acting bacterial mutagenicity [3, 4, 8]. It is well established that, NPAH isomers with the nitro group perpendicular to the plane of the aromatic moiety exhibit lower mutagenic activity than that of the corresponding planar homologues [3, 4, 8].

Among NPAH compounds, nitrobenzo[*a*]pyrenes (NB*a*Ps) constitute a representative group characterized by different biological activities as a function of the nitro substituent position [1–4, 8–17]. In fact, as documented in the literature, both 1- and 3-NB*a*Ps are powerful direct-acting and S9-activated mutagens in Salmonella typhimurium [1–3, 11–17]. Additionally, they are moderate mutagens in S9-mediated Chinese Hamster Ovary Cell hprt assay [13]. By contrast 6-NB*a*P isomer does not exhibit significant direct-acting

mutagenic potencies [1–3, 11, 12, 14–17]. Experimental structure is available only for 6-NB*a*P isomer from X-Ray diffraction measurements [18], while recently, theoretical geometries of 1-, 3- and 6-NB*a*P isomers have been computed by using density functional theory (DFT) [19]. Observed IR and Raman spectra of 1-, 3- and 6-NB*a*P have been recorded in both solid (KBr) and solution (CCl_4) phases [19] and also for 6-NB*a*P in many other solvents [8]. In addition, UV-vis absorption, mass, ^1H and ^{13}C NMR spectra were previously reported in the literature [3, 19, 20]. Both experimental and theoretical studies concordantly predict that for 1- and 3-NB*a*P isomers the nitro group is planar or near planar with respect to the aromatic system [3, 8, 10, 19]. On the other hand, both the observed [18] and computed [10, 19] structure of 6-NB*a*P isomer exhibits the nitro substituent perpendicular or almost perpendicular due to the presence of two hydrogen atoms in peri position. This structural arrangement of the nitro group has been hypothesized to be a major cause of an ineffective binding of 6-NB*a*P to the nitroreductase enzyme, inhibiting its mutagenic capacity [9]. As reported in the literature, proposed metabolic activation pathways of NB*a*Ps principally consist in ring oxidation reactions under aerobic conditions, nitroreduction processes under anaerobic conditions or combinations of oxidation and reduction reactions [4, 21, 22]. These processes are usually preceded by penetration of the NPAH into the cellular system, diffusion and binding to the active site of the specific enzyme [22]. In particular, the last step may be controlled by intermolecular interactions, which depend on dipole moment and polarizability of the system.

Thus, in order to understand the role of the individual processes involved in the metabolic activation mechanism of DNA and to predict the mutagenic activities of NB*a*Ps, may be useful to determine related chemical-physical properties such as structure, ionization potential (IP), electron affinity (EA), dipole moment (μ), electronic polarizability (α), through computational methods. In the present work we report accurate theoretical calculations of IP, EA, μ and α of 1-, 3- and 6-NB*a*P isomers (Fig. 1) to investigate the effect of the nitro substitution on these properties and explore possible relationships with mutagenic activities. To this purpose we employed the DFT-B3LYP functional [23, 24] and the recent semiempirical PM6 method [25].

Computational details

Equilibrium geometries of NB*a*P isomers recently determined at the B3LYP/6-311++G** level [19] were used throughout this work. These structures are stationary points on the potential energy surface since all the harmonic

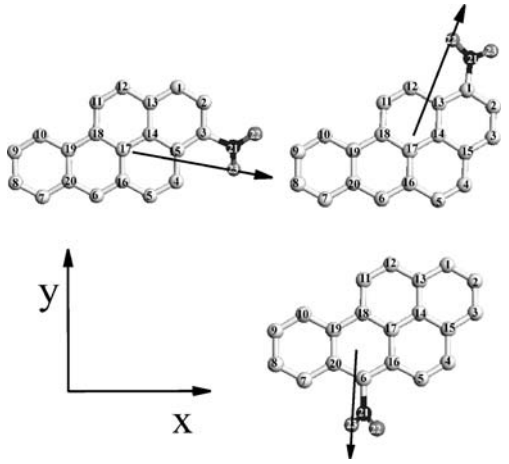

Fig. 1 Structure, atomic numbering and dipole moment vector of nitrobenzo[*a*]pyrene isomers

vibrational frequencies are positive [19]. Computed μ values and atomic charges (q) of the neutral ground state were obtained at the B3LYP level with 6-31+G* basis set [26], which includes both polarized *d* and diffuse *s* and *p* functions on the carbon, oxygen and nitrogen atoms. Use of flexible basis set including polarized and diffuse functions is necessary to adequately describe diffuse regions of the charge distribution [26]. Atomic charges were evaluated by means of the natural population atomic (NPA) scheme [27], which is recognized to be almost independent on basis set choice [28]. Static electronic dipole polarizability components (α_{ij}, i=x, y, z) were calculated through two different approaches: (a) at semiempirical PM6 level [25] recently implemented in the MOPAC2007 package [29] as the second derivative of electronic energy (E) with respect to electric field strength components (F_i) [30]:

$$E(F) = E(0) - \sum_i \mu_i F_i - 1/2 \sum_{ij} \alpha_{ij} F_i F_j - \ldots \quad (1)$$

$$\alpha_{ij} = - \left[\frac{\partial^2 E(F)}{\partial F_i \partial F_j} \right]_{F \to 0} \quad (2)$$

(b) at semiempirical ZINDO/S [31] level using the following sum-over-states (SOS) expression [32]:

$$\alpha_{ii} = 2 \sum_n \frac{(M_i^{ng})^2}{E^{ng}} \quad (3)$$

where E^{ng} is the energy difference between the neutral ground and the nth electronic excited state and M_i^{ng} is the corresponding i-component of the transition moment.

Polarizability is usually expressed as averaged polarizability (<α>) and polarizability anisotropy (Δα):

$$< \alpha > = \frac{1}{3}\left(\alpha_{xx} + \alpha_{yy} + \alpha_{zz}\right) \quad (4)$$

$$\Delta\alpha = \left\{\frac{1}{2}\left[\left(\alpha_{xx} - \alpha_{yy}\right)^2 + \left(\alpha_{xx} - \alpha_{zz}\right)^2 + \left(\alpha_{yy} - \alpha_{zz}\right)^2\right]\right\} \quad (5)$$

Vertical first IP and EA values were calculated at the B3LYP/6-31+G* level through a ΔSCF procedure as:

$$IP = E_{cation} - E_{neutral} \quad (6)$$

$$EA = E_{neutral} - E_{anion} \quad (7)$$

where E_{cation}, $E_{neutral}$ and E_{anion} are single point total energy of the cation, neutral and anion states, respectively, at the optimized neutral ground state geometry. For neutral ground state we used restricted B3LYP functional (RB3LYP) to compute the total energy, while for radical cation and anion states unrestricted B3LYP function (UB3LYP) was adopted. Note that, for all cases UB3LYP method gave only a negligible spin contamination ($S^2 \sim 0.75$). UB3LYP/6-31+G* method have been recently employed with success in predicting experimental EA values of many PAHs [33] and isothiocyanates [34].

Conversion factors to SI units are: energy (E), 1 Hartree = $4.3597482 \times 10^{-15}$ J; dipole moment (μ), 1 D = 3.33564×10^{-30} Cm; dipole polarizability (α), 1 a.u. = 1.648778×10^{-41} $C^2m^2J^{-1}$.

All calculations were performed with GAUSSIAN 03 [35], GAMESS [36] and MOPAC 2007 [29] series of programs.

Results and discussion

Geometries and relative energies

Structures of 1-NB*a*P, 3-NB*a*P and 6-NB*a*P isomers as well as those of the reference compounds nitrobenzene (NB) and benzo[*a*]pyrene (B*a*P) have been recently optimized at the DFT-B3LYP level with the 6-311+G* basis set [19] and are used in the present work. As can be seen in Fig. 1, for 6-NB*a*P isomer, DFT computations [19] predict O_{22}-N_{21}-C_6-C_{16} and O_{23}-N_{21}-C_6-C_{20} dihedral angles of 62.6 and 62.8°, respectively, in good agreement with observed values of 68.5 and 70.6° obtained from X-ray diffraction experiments [18]. The large values of the O-N-C-C dihedral angles of 6-NB*a*P are due to the remarkable steric hindrance of the nitro group with both the hydrogen atoms in peri position as shown in Fig. 1. On the other hand, for both 1-NB*a*P and 3-NB*a*P isomers, DFT calculations predict smaller O-N-C-C dihedral angles being close to 30° [19]. Therefore on

Table 1 Relative energy, ΔE (kcal mol^{-1}), HOMO and LUMO eigenvalues, ε_{HOMO} (eV) and ε_{LUMO} (eV), first ionization potential, IP (eV), electron affinity, EA (eV), hardness, η (eV) and electrophilic index, ω (eV) of 1-, 3-and 6-nitrobenzo[*a*]pyrene isomers, 1- and 2-nitronaphthalene isomers, benzo[*a*]pyrene and nitrobenzene[a]

	1-NB*a*P	3-NB*a*P	6-NB*a*P	1-NN		2-NN		B*a*P		NB	
				Calc.	Exp.	Calc.	Exp.	Calc.	Exp.	Calc.	Exp.
ΔE[b]	0.00	0.25	4.05								
ε_{HOMO}[c]	−7.34	−7.33	−7.38	−8.64		−8.64		−6.77		−10.10	
ε_{LUMO}[c]	0.24	0.29	0.49	0.70		0.75		1.16		0.86	
IP	7.27	7.25	7.23	8.52	8.59[d]	8.55	8.63[d]	6.79	7.12[e]	9.99	9.92[f]
EA	1.58	1.55	1.34	1.13	1.23[g]	1.10	1.18[g]	0.65	0.81[h]	0.88	1.00[i]
η[j]	2.85	2.85	2.95	3.69	3.68	3.72	3.72	3.07	3.16	4.56	4.46
ω[k]	3.44	3.40	3.12	3.15	3.28	3.12	3.23	2.25	2.49	3.24	3.34

[a] B3LYP/6-31+G* results
[b] B3LYP/6-31+G*//B3LYP/6-311+G* total electronic energy value of 1-NB*a*P is computed to be −973.941981 Hartrees. PM6//B3LYP/6-311+G* ΔE values for 1-, 3- and 6-NB*a*P isomers are 0.04, 0.00 and 2.58 kcal mol^{-1}, respectively
[c] HF/6-31+G* results
[d] Photoelectron spectroscopy, from ref. [48].
[e] Photoelectron spectroscopy, from ref. [46]
[f] Photoelectron spectroscopy, from ref. [44]
[g] Temperature dependent equilibrium ion/molecule reaction, from ref. [43]
[h] Laser photoelectron spectroscopy, from ref. [47]
[i] Ion-molecule reaction equilibrium method, from ref. [45]
[j] Data obtained through Eq. (8) using IP and EA values
[k] Data obtained through Eq. (9) using IP and EA values

passing from 1-NB*a*P (or 3-NB*a*P) to 6-NB*a*P the π-conjugation between the nitro group and the aromatic system is reduced as also pointed out by an increase of the C-N bond length by ca 0.007 Å [19]. As a consequence, for 6-NB*a*P the partial loss of π-delocalization determines a greater destabilization with respect to the more conjugate isomers. Indeed, 6-NB*a*P is predicted to be 4.05 and 2.54 kcal mol^{-1} less stable than 1-NB*a*P isomer by present B3LYP/6-31+G* and PM6 calculations (Table 1), respectively, while as expected, 1- and 3-NB*a*P isomers are almost isoenergetic (ΔE=0.25 and −0.04 kcal mol^{-1}, respectively).

Electron affinities

As reported in the literature, oxidative, reductive or combinations of oxidative and reductive reactions are the proposed mutagenic mechanisms of DNA involving NB*a*Ps [4, 21, 22]. Thus, in order to obtain much more insight into mutagenic properties of NB*a*P isomers we calculated vertical ΔSCF IP and EA, the B3LYP/6-31+G* values being reported in Table 1 together with those of NB, B*a*P as well as nitronaphthalene (NN) isomers for comparison. In addition, in the Table we included the lowest unoccupied molecular orbital (LUMO) and highest occupied molecular orbital (HOMO) eigenvalues (ε_{LUMO} and ε_{HOMO}, respectively) obtained at the HF/6-31+G* level, which through the Koopmans' theorem can be connected to EA and IP values (IP≈-ε_{HOMO}, EA≈-ε_{LUMO}), respectively [37]. Quantitative structure activity relationship (QSAR) approaches, using computed ε_{LUMO} values which can be related to half-wave reduction potentials, were previously employed to elucidate mutagenic behaviour on series of NPAHs with different molecular size and structure [22, 38–42]. It is important to point out that, suitable correlations of mutagenic activity with the combination of nitro-group orientation and electronic properties (such as first half-wave reduction potential) should be performed among structurally similar compounds [2]. However, while ε_{LUMO}/mutagenic activity relationship holds reasonably well for the series of nitroanthracenes and nitrophenanthrenes [41] and mononitrobenzanthrones [42], on the other hand it fails for polynitrobenzanthrones [42], nitronaphthalenes and especially for nitropyrene isomers [41]. Additionally, previous ε_{LUMO}/mutagenic activity relationships often used ε_{LUMO} data obtained at semiempirical level [22, 40, 42], which in some cases gave unreliable EA predictions for NPAH isomers. For example, in the case of prototypical NN isomers, AM1 ε_{LUMO} values were computed to be −1.266 and −1.415 eV for 1-NN and 2-NN isomers, respectively, [22], which disagree with the experimental EA values of 1.23 and 1.18 eV, respectively [43]. Use of the DFT-ΔSCF approach is expected to give quantitative EA predictions much more adequately than -ε_{LUMO} values. To our knowledge, both experimental and theoretical IP and EA values of NB*a*Ps are lacking, while observed values for the reference compounds NB [44, 45], B*a*P [46, 47], 1-NN and 2-NN [43, 48] are available from the literature. Present B3LYP/6-31+G* EA values reproduce reasonably well the experimental figures of NB, B*a*P and NNs, with deviation within 0.08–0.16 eV. It is worth to note that, the calculated EA data of NN isomers are close to each other, in agreement with experiment. Introduction of the strong electron withdrawing nitro group to the B*a*P moiety increases EA value by 0.69–0.93 eV. As a consequence, for all NB*a*P isomers, EA value is significantly positive, indicating that the anionic state is very stable. A graphical representation of the π* LUMO of 1- and 6-NB*a*P isomers obtained at the HF/6-31+G* level is reported in Fig. 2. For both the isomers LUMO is mainly localized over the nitro group, with a stabilizing contribution in the region of the C-N bond. This implies that, the higher the O-N-C-C dihedral angle the greater the destabilization of ε_{LUMO}. Indeed on passing from 1- to 6-NB*a*P isomer ε_{LUMO} increases by 0.25 eV, becoming more positive. A similar variation is obtained for EA values which are computed to be 1.58 and 1.34 eV for 1- and 6-NB*a*P, respectively. On the other hand, EA and ε_{LUMO} values of 1- and 3-NB*a*P are close to each other. It is interesting to notice that, present results are consistent with the mutagenic activity of NB*a*Ps obtained using the Salmonella typhimurium bacterial strains TA98 [49, 50], TA100 [49, 50] and YG1024 [51], which increase by about two orders of magnitude on passing from 6- to 3-NB*a*P [3, 8, 15–17], thus supporting the proposed nitro-reduction pathway [4, 21, 22], which may be considered, especially within an anaerobic context, a critical step in formation of DNA adducts with metabolites of NB*a*Ps. On the other hand, the very close EA value of 1- and 3-NB*a*Ps

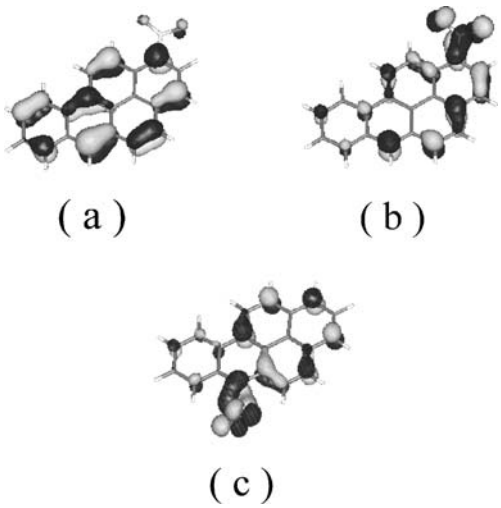

Fig. 2 HF/6-31+G* HOMO (**a**) and LUMO (**b**) of 1-nitrobenzo[*a*]pyrene and LUMO (**c**) of 6-nitrobenzo[*a*]pyrene isomer

does not allow to elucidate their direct-acting mutagenicity, which is however, rather uncertain, being similar for TA100 (2376 and 3119 revertants/nmol, respectively) and YG1024 (7700, 6500 revertants/nmol, respectively) strains [15, 16] but different for TA98 strain (650, 1370 revertants/nmol, respectively [15] and 713, 1931 revertants/nmol, respectively [16]). Additionally, we note that EA values of NB*a*Ps are, 0.2–0.5 eV higher than those of NNs computed at the same level of theory, in agreement with the noticeably greater mutagenic potencies of the former with respect to the latter (by 3–5 orders of magnitude) [52].

Atomic charges and ionization energies

Table 2 lists the atomic charges based on the NPA scheme. In agreement with experimental evidences, the results show that especially for 1- and 3-NB*a*Ps, carbon atom at position 8 (see Fig. 1) is the most preferred site for oxidative attack, leading to formation of epoxide intermedium [4]. Note also that atomic charges at carbon atoms C_7, C_9 and C_{10} are significantly negative, confirming that subsequent oxidative attacks preferentially involve the terminal benzene ring [4]. First IP is defined as the amount of energy necessary to extract an electron. As can be seen in Table 1, the observed IP values of NB and NN isomers are adequately predicted by B3LYP/6-31+G* calculations with deviations within 0.07–0.08 eV (0.8–0.9 %). By contrast, present computations underestimate the experimental IP value of B*a*P by 0.33 eV (4.6%). Differently from EA, IP value of NB*a*P isomers is almost unaffected by the substituent position, being computed in the 7.23–7.27 eV range. Thus oxidative mechanisms are expected to be rather similar for each NB*a*P isomer. This result is also confirmed by the energy gain for the carbocation formation from the diol-epoxide intermedium, which is predicted to be in the 226–228 kcal mol^{-1} range for 1-, 3- and 6-NB*a*P derivatives by B3LYP/6-31G* calculations.

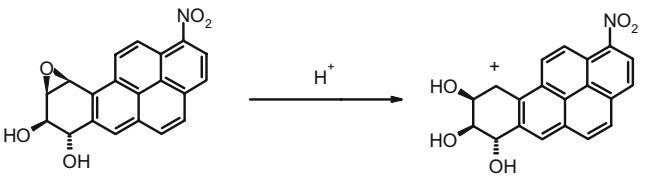

In Fig. 2 we report a graphical representation of the π HOMO of 1-NB*a*P isomer evaluated at the HF/6-31+G* level. As shown in Fig. 2, HOMO is localized on the B*a*P framework. Introduction of nitro group increases IP value by 0.44–0.48 eV, indicating that, at variance of nitro-reduction, the oxidation step in the case of NB*a*P is much less favourable than for BaP. Therefore, the observed noticeably higher carcinogenic potency of BaP in comparison to NB*a*Ps [2], might be related to its lower IP value, which encourages oxidative pathways.

Hardness and electrophilicity index

Molecular hardness (η) and electrophilicity index (ω) are generalized molecular parameters widely used to explore and compare stability and reactivity properties of series of compounds [53, 54]. Typical working formulas for the calculation of η, and ω values may be determined by using the finite difference approximation [53]:

$$\eta = (\mathrm{IP} - \mathrm{EA})/2 \tag{8}$$

$$\omega = \frac{(\mathrm{IP} + \mathrm{EA})^2}{4(\mathrm{IP} - \mathrm{EA})}. \tag{9}$$

Table 1 shows η and ω values of NB, B*a*P, NNs and NB*a*P isomers using IP and EA data. Hardness decreases on passing from 6- to 3-NB*a*P isomers by 0.1 eV, then remaining constant between 3- and 1-NB*a*P isomer. These results are in apparent contrast with the relative stability, the maximum hardness principle (MHP) which establishes that a molecular system tends towards a state of maximum hardness [54], being not satisfied. Note that there are other cases in the literature involving isomers and conformers of organic compounds, where the MHP does not always hold [55–58]. Additionally, as can be seen from Table 1, ω value increases in the order:

$$\mathrm{B}a\mathrm{P} < 6-\mathrm{NB}a\mathrm{P} \sim 2-\mathrm{NN} \sim 1-\mathrm{NN} < \mathrm{NB} < 3-\mathrm{NB}a\mathrm{P} \sim 1-\mathrm{NB}a\mathrm{P},$$

this sequence being principally determined by the EA values. Note the lower electrophilic character of the 6-NB*a*P isomer in comparison to NB.

Dipole moments

Dipole moment is a vectorial property which represents the charge distribution in a molecule. It may contribute to intermolecular interactions, through both electrostatic and inductive terms [59]. In Table 2 are reported μ values computed at the B3LYP/6-31+G* as well as semiempirical PM6 level. For NB is available a gas-phase experimental datum (4.22 D) [60]. Both B3LYP/6-31+G* and PM6 computations overestimate the experimental datum by 0.74 D (+18%) and 1.12 D (+27%), respectively. In all cases, PM6 systematically overestimates B3LYP/6-31+G* data. For NB*a*P series the sequence of μ value is (in

parentheses is given the B3LYP/6-31+G* value expressed in D):

$$6-\mathrm{NB}a\mathrm{P}\ (4.97) < 1-\mathrm{NB}a\mathrm{P}\ (6.36) < 3-\mathrm{NB}a\mathrm{P}\ (6.48)$$

The largest variation is obtained from 6- to 3-NB*a*P which at the B3LYP/6-31+G* level is computed to be 1.51 D (+30%). On the other hand 1- and 3-NB*a*P isomers show much closer μ values to each other (within 0.12 D). These results are in line with previous HF/6-31G* calculations on NB, where μ value is reduced by 0.48 D (10%) when passing from the planar structure (C_{2v} symmetry) to that with the nitro group perpendicular to the benzene ring (C_s symmetry) [61]. As can be seen in Fig. 1, for all NB*a*P isomers, μ vector is substantially directed along the C-N bond. Atomic charge over the nitro group (qNO_2) evaluated within the NPA approximation (Table 2) is large and negative consistently with the highly polar structures. Specifically qNO_2 charges of 1- and 3-NB*a*P isomers are very close to each other, while that of 6-NBaP isomer is ca. 0.04 e more positive, in agreement with the corresponding μ values. Note that, even if BaP is a non polar compound (μ=0.01–0.02 D), the charge distribution over C atoms is substantially similar to that of the NB*a*P isomers.

Polarizabilities and electronic excitations

For atoms and molecules the electronic polarizability tensor represents a measure of the change of the electronic density under application of external electric fields. As for μ, also α may contribute to enzyme-ligand interactions, through both inductive and dispersive phenomena [59, 62–66]. Additionally, there are some indications showing that electronic polarizability might be related to hydrophobicity [67], which was found to be crucial for the description of the mutagenic activity of a large series of NPAH compounds [22, 40]. In Table 3 we report static electronic dipole polarizabilities computed at the PM6 and SOS-ZINDO/S levels. For NB are available experimental values of 87 and 90 a.u. measured in DMSO and hexane solutions, respectively [68]. Present PM6 value of 86 a.u. compares reasonably well with both experimental data as well as with the highest-level theoretical estimate of 88 a.u. computed at correlated ab initio MP2 level with the

Table 2 Dipole moment μ (D) and natural population atomic charges (e) of, 1-, 3-, 6-nitrobenzo[*a*]pyrene isomers, benzo[*a*]pyrene and nitrobenzene[a]

	1-NB*a*P	3-NB*a*P	6-NB*a*P	B*a*P	NB
μ	6.36 (6.97)	6.48 (7.05)	4.97 (6.05)	0.02 (0.01)	4.96 (5.34) [b]
C_1	0.06890	−0.21108	−0.20172	−0.21169	0.05758
C_2	−0.20667	−0.21598	−0.23468	−0.23696	−0.21316
C_3	−0.22784	0.06940	−0.20937	−0.22269	−0.23602
C_4	−0.23605	−0.23474	−0.19463	−0.22678	
C_5	−0.16886	−0.16654	−0.21543	−0.19073	
C_6	−0.15623	−0.15232	0.08834	−0.17381	
C_7	−0.21294	−0.21163	−0.26702	−0.21638	
C_8	−0.23637	−0.23657	−0.22626	−0.24061	
C_9	−0.22684	−0.22707	−0.22925	−0.23589	
C_{10}	−0.21959	−0.22018	−0.22247	−0.21982	
C_{11}	−0.18169	−0.17550	−0.22943	−0.19176	
C_{12}	−0.19696	−0.21808	−0.16874	−0.21213	
C_{13}	−0.03514	−0.04731	−0.07940	−0.06893	−0.21316
C_{14}	−0.01616	−0.00603	−0.00760	−0.01038	−0.23602
C_{15}	−0.00823	−0.01408	−0.04006	−0.03659	−0.2072
C_{16}	−0.06230	−0.06482	−0.07219	−0.05647	
C_{17}	−0.02082	−0.01509	−0.00656	−0.01721	
C_{18}	−0.03110	−0.03128	−0.00950	−0.02911	
C_{19}	−0.02042	−0.02038	−0.06300	−0.02763	
C_{20}	0.24118	−0.05313	0.12129	−0.05018	
N_{21}	0.49283	0.49316	0.49287		0.49497
O_{22}	−0.39097	−0.38595	−0.36578		−0.38103
O_{23}	−0.38810	−0.38944	−0.36511		−0.38103

[a] B3LYP/6-31+G* results. Value in parentheses refers to PM6 computation. For atomic numbering see Fig. 1
[b] Experimental gas-phase value is 4.22 D, from ref. [60]

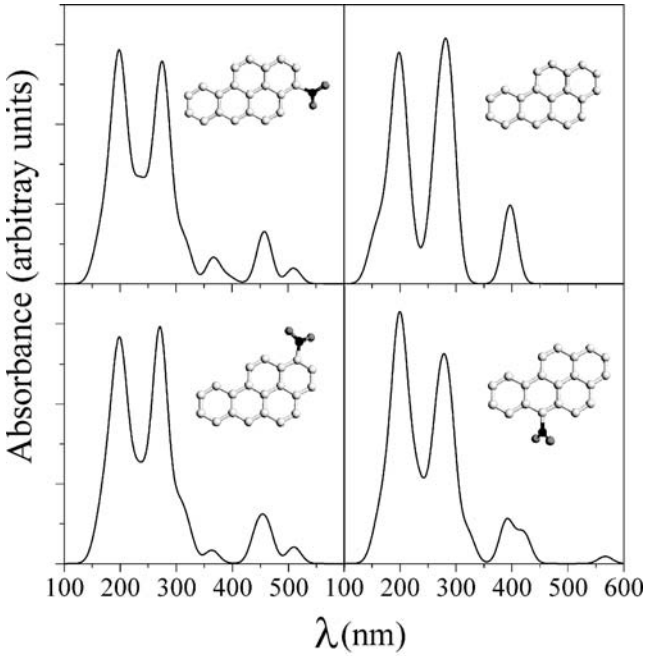

Fig. 3 Calculated ZINDO/S low energy absorption spectrum of benzo[*a*]pyrene and nitrobenzo[*a*]pyrene isomers. Gaussian line shapes with halfwidth of 20 nm are used

polarized and diffuse [5s3p2d/3s2p] Sadlej basis set, specifically developed for polarizability calculations [69]. To our knowledge both experimental and theoretical polarizability data of B*a*P and NB*a*Ps are unavailable. The SOS-ZINDO/S approximation which in the present case is restricted to the hundred lowest-energy singlet excited states predict <α> values for NB*a*P isomers in the 222–239 a.u. range, which are systematically lower than the corresponding obtained at the PM6 level (276–282 a.u.). However, SOS approach is here employed in a comparative way in order to explore the most contributing excited states to the electronic polarizabilities. Vertical singlet electronic excited states of B*a*P and NB*a*P isomers were determined at the ZINDO/S level and the spectra in the 100–600 nm wavelength range are depicted in Fig. 3. Computed absorption spectra of 1- and 3-NB*a*P isomers are similar to each other, while the spectrum of 6NB*a*P resembles that of B*a*P, in reasonable agreement with experiment [3]. As can be seen in Table 3, 1- and 3-NB*a*P isomers show an analogue <α> value, while they are more polarizable than 6-NB*a*P by 5-6 a.u. at the PM6 level, in line with a greater π-delocalization, but in disagreement with the minimum polarizability principle (MPP), which establishes that a molecular system tends towards a state of minimum polarizability [70]. These results are consistent with those obtained for the molecular hardness. It is worth mentioning that, in the present case, π-conjugative contributions dominate over thermodynamic stability effects in the determination of the polarizability values as previously found in other π-conjugated systems [55, 58, 71]. Additionally, the above results are in some consistency with previous HF/6-31G* polarizability computations on the planar equilibrium geometry NB and its corresponding structure with the nitro group perpendicular to the benzene ring [61]. In fact, the former is predicted to be more polarizable than the latter form by 7.4 a.u. (8%). Present calculations show that introduction of nitro group increases PM6 <α> value of B*a*P by 20-26 a.u. (8–10%). For all isomers and especially for 3-NB*a*P, α_{xx} is the largest component within our choice of coordinate (Fig. 1), being ca. 50% of the sum of the diagonal $\alpha_{xx} + \alpha_{yy} + \alpha_{zz}$ components. The sequence of α_{xx} computed at the PM6 level is (in parentheses is reported the value expressed in a.u.):

$$6-\text{NB}a\text{P}\ (416) < 1-\text{NB}a\text{P}\ (433) < 3-\text{NB}a\text{P}\ (450).$$

A similar order is also obtained for $\Delta\alpha$, the corresponding values being calculated to be 317, 364 and 402 a.u., respectively. On passing from 6-NBaP to 3-NBaP α_{xx} and $\Delta\alpha$ values increase by 8 and 27%, respectively. It is worth noting that, the above results are consistent with the previous conclusions traced by Yu et al. [72], for which direct-acting TA98 mutagenicity is maximized for NPAH geometric isomers with the nitro group located at the longest molecular axis. According to the SOS formula (Eq. 3), for all NBaP isomers the largest contribution to α_{xx}

Table 3 Static electronic dipole polarizabilities α (a.u.) of benzo[*a*]pyrene, nitrobenzene, 1-, 3- and 6-nitrobenzo[*a*]pyrene isomers[a]

	1-NB*a*P		3-NB*a*P		6-NB*a*P		B*a*P		NB	
	PM6	SOS-ZINDO/S	PM6	SOS-ZINDO/S	PM6	SOS-ZINDO/S	PM6	SOS-ZINDO/S	PM6	SOS-ZINDO/S
α_{xx}	433	424	450	474	416	392	401	389	103	82
α_{yy}	291	282	275	232	278	246	255	216	111	89
α_{zz}	120	10	121	10	133	28	112	6	43	6
<α>	282	239	282	239	276	222	256	204	86(87,90)[b]	59
Δα	271	364	285	402	245	317	250	332	64	80

[a] For the description of the coordinate system orientation see Fig. 1
[b] Values in parentheses refer to experimental data in DMSO and hexane solution, respectively, from ref. [68]

(20–30%) is provided by the intense π–π* HOMO-1→LUMO+1 excitation placed at 4.50, 4.45 and 4.27 eV for 1-, 3-, and 6-NBaP isomers, respectively (λ=276, 279, and 290 nm, respectively). In addition we note that 3-NB*a*P exhibits another noticeable contribution (19%), given by the HOMO→LUMO excitation at 2.70 eV (459 nm). The corresponding excitation for 1- and 6-NB*a*P isomers gives a minor contribution to α_{xx} value (7 and 8%, respectively).

The results obtained from the μ and α calculations indicate that, the capacity of 1- and 3-NB*a*P isomers to bind to enzymes involved in the mutagenic pathways should be greater than that of 6NB*a*P isomer, in consistency with their significant different mutagenic activities [3, 8, 15–17]. Recently, the different mutagenic behaviour of 1- and 2-NN isomers has been elucidated on the basis of electron charge distributions described by IR and Raman intensities of vibrations mainly localized on the nitro group [73]. Additionally, both μ and α_{xx} values of 3-NB*a*P are larger than those of 1-NB*a*P isomer, although the variations are small (2 and 4%, respectively). Anyway, these results are in qualitative agreement with the observed mutagenic capacities, the values for 3-NB*a*P being close or greater than those for 1-NB*a*P isomer [15, 16].

Conclusions

The results obtained herein allow us to conclude that the significant observed mutagenic activity difference between 6- and 3-NB*a*P (or 1-NB*a*P) can be related to their different electronic properties. Both the enzyme-substrate binding capacity through dipole moment and electronic polarizability terms and the nitroreductive process through EA contribute to the mutagenic potency of NB*a*P isomers. On the other hand, IP values are predicted to be close for the investigated isomers, suggesting that oxidative pathways should not be critical for the different mutagenic behaviour of this series of NPAH compounds.

Acknowledgements This work was carried out in the framework of the RIC action of the Project No. 1999/IT.16.1.PO.011/3.13/7.2.4/339 PROT. 238, "Formazione per la ricerca nel campo della bonifica dei siti contaminate" POR Sicilia 2000–2006, Asse: III Misura: 3.13.

References

1. Tokiwa H, Ohnishi Y (1986) Crit Rev Toxicol 17:23–60
2. Fu PP (1990) Drug Metab Rev 22:209–268
3. Chou MW, Heflich RH, Casciano DA, Miller DW, Freeman JP, Evans FE, Fu PP (1984) J Med Chem 27:1156–1161
4. Zhan D-J, Chiu L-H, Von Tungeln LS, Herreno-Saenz D, Cheng E, Evans FE, Heflich RH, Fu PP (1997) Mutat Res 379:43–52
5. Spain JC (1995) Ann Rev Microbiol 49:523–555
6. Parales RE, Ditty JL (2005) Curr Opin Biotechnol (2005) 16:315
7. Friemann R, Ivkovic-Jensen MM, Lessner DJ, Yu CL, Gibson DT, Parales RE, Eklund H (2005) J Mol Biol 348:1139–1151
8. Li YS, Fu PP, Church JS (2000) J Mol Struct 550–551:217–223
9. Pitts JN, Lokensgard DM, Harger W, Fisher TS, Mejia V, Schuler JJ, Scorziell GM, Katzenstein YA (1982) Mutat Res 103:241–249
10. Fukuhara K, Kurihara M, Miyata N (2001) J Am Chem Soc 123:8662–8666
11. Colvert KK, Fu PP (1986) Biochem Biophys Res Commun 141:245–250
12. Heflich RH, Unruh LE, Thornton-Manning JR, Von Tungeln LS, Fu PP (1989) Mutat Res 225:157–163
13. Hass BS, Heflich RH, Scho HM, Chou MW, Fu PP, Casciano DA (1986) Carcinogenesis 7:681–684
14. Horikawa K, Sera N, Murakami K, Sano N, Izumi K, Tokiwa H (1998) Toxicol Lett 98:51–58
15. Sera N, Kai M, Horikawa K, Fukuhara K, Miyata N, Tokiwa H (1991) Mutat Res 263:27–32
16. Jung H, Shaikh AU, Heflich RH, Fu PP (1991) Environ Mol Mutagen 17:169–180
17. Ishii S, Hisamatsu Y, Inazu K, Kobayashi T, Aika K-I (2000) Chemosphere 41:1809–1819
18. Warner SD, Lebuis A-M, Farant J-P, Butler IS (2003) J Chem Cryst 33:213–217
19. Onchoke KK, Hadad CM, Dutta PK (2006) J Phys Chem A 110:76–84
20. Dyker G, Kadzimirsz D, Thoene A (2003) Eur J Org Chem 16:3162–3166
21. Vance WA, Okamoto HS, Wang YY (1988) In: King CM, Romano LJ, Schuetzle D (eds) Carcinogenic and mutagenic responses to aromatic amines and nitroarenes. Elsevier, New York, pp 291–302
22. Debnath AK, Lopez de Compadre RL, Debnath G, Shusterman AJ, Hansch C (1991) J Med Chem 34:786–797
23. Becke AD (1993) J Chem Phys 98:1372–1377
24. Lee C, Yang AD, Parr RG (1988) Phys Rev B 37:785–789
25. Stewart JJP (2007) J Mol Model 13:1173–1213
26. Hehre WJ, Radom L, Schleyer PvR, Pople JA (1986) Ab initio molecular orbital theory. Wiley, New York
27. Reed AE, Curtiss LA, Weinhold F (1988) Chem Rev 88:899, and references therein
28. De Proft F, Martin JML, Geerlings P (1996) Chem Phys Lett 250:393–401
29. Stewart JJP, MOPAC 2007, Stewart Computational Chemistry, Colorado Springs, CO, USA, http://OpenMOPAC.net
30. Karna SP, Dupuis M (1991) J Comput Chem 12:487–504
31. Zerner MC (1991) In: Lipkowitz KB, Boyd DB (eds) Review computational chemistry, Vol. 2. VCH, New York, pp 313–366
32. Orr BJ, Ward JF (1971) Mol Phys 20:513–526
33. Modelli A, Mussoni L, Fabbri D (2006) J Phys Chem A 110:6482–6486
34. Modelli A, Jones D (2006) J Phys Chem A 110:13195–13201
35. Frisch MJ, Trucks GW, Schlegel HB, Scuseria GE, Robb MA, Cheeseman JR, Montgomery JA Jr, Vreven T, Kudin KN, Burant JC, Millam JM, Iyengar SS, Tomasi J, Barone V, Mennucci B, Cossi M, Scalmani G, Rega N, Petersson GA, Nakatsuji H, Hada M, Ehara M, Toyota K, Fukuda R, Hasegawa J, Ishida M, Nakajima T, Honda Y, Kitao O, Nakai H, Klene M, Li X, Knox JE, Hratchian HP, Cross JB, Bakken V, Adamo C, Jaramillo J, Gomperts R, Stratmann RE, Yazyev O, Austin AJ, Cammi R, Pomelli C, Ochterski JW, Ayala PY, Morokuma K, Voth GA, Salvador P, Dannenberg JJ, Zakrzewski VG, Dapprich S, Daniels AD, Strain MC, Farkas O, Malick DK, Rabuck AD, Raghavachari K, Foresman JB, Ortiz JV, Cui Q, Baboul AG, Clifford S, Cioslowski J, Stefanov BB, Liu G, Liashenko A, Piskorz P, Komaromi I, Martin RL, Fox DJ, Keith T, Al-Laham MA, Peng CY, Nanayakkara A, Challacombe M, Gill PMW, Johnson B,

Chen W, Wong MW, Gonzalez C, Pople JA (2003) Gaussian 03, Revision B.03. Gaussian Inc, Pittsburgh PA
36. Schmidt MW, Baldridge KK, Boatz JA, Elbert ST, Gordon MS, Jensen JH, Koseki S, Matsunaga N, Nguyen KA, Su S, Windus TL, Dupuis M, Montgomery JA Jr (1993) J Comput Chem 14:1347–1363
37. Koopmans T (1933) Physica 1:104–113
38. Klopman G, Tonucci DA, Holloway M Rosenkranz HS (1984) Mutat Res 126:139–144
39. Maynard AT, Pedersen LG, Posner HS, McKinney JD (1986) Mol Pharmacol 29:629–636
40. Lopez de Compadre RL, Shusterman AJ, Hansch C (1988) Int J Quantum Chem 34:91–101
41. Onchoke KK, Hadad CM, Dutta PK (2004) Polycyclic Aromat Compd 24:37–64
42. Takamura-Enya T, Suzuki H, Hisamatsu Y (2006) Mutagenesis 21:399–404
43. Heinis T, Chowdhury S, Kebarle P (1993) Org Mass Spectrom 28:358–365
44. Akiyama I, Li KC, LeBreton PR, Fu PP, Harvey RG (1979) J Phys Chem 83:2997–3003
45. Desfrancois C, Periquet V, Lyapustina SA, Lippa TP, Robinson DW, Bowen KH, Nonaka H (1999) J Chem Phys 111:4569–4576
46. Kimura K, Katsumata S, Achiba Y, Yamazaki T, Iwata S (1981) In: Handbook of HeI Photoelectron Spectra of Fundamental Organic Compounds. Ionization energies, Ab initio assignments, and valence electronic structure for 200 molecules. Japan Scientific Soc. Press, Tokyo
47. Crocker L, Wang TB, Kebarle P (1993) J Am Chem Soc 115:7818–7822
48. Klasinc L, Kovac B, Guesten H (1983) Pure Appl Chem 55:289–298
49. Ames BN, McCann J, Yamasaki E (1975) Mutat Res 31:347–364
50. Maron DM, Ames BN (1983) Mutat Res 113:173–215
51. Watanabe M, Ishidate Jr M, Nohmi T (1990) Mutat Res 234:337–348
52. Rosenkranz HS, Mermelstein R (1983) Mutat Res 114:217–267
53. Chattaraj PK, Sarkar U, Roy DR (2006) Chem Rev 106:2065–2091, and references therein
54. Pearson RG (1993) Acc Chem Res 26:250–255
55. Torrent-Sucarrat M, Luis JM, Duran M, Solà M (2001) J Am Chem Soc 123:7951–7952
56. Senthilkumar K, Kolandaivel P (2003) Comput Biol Chem 27:173–183
57. Selvarengan P, Kolandaivel P (2005) Bioorg Chem 33:253–263
58. Alparone A, Millefiori A, Millefiori S (2005) Chem Phys 312:261–274
59. Staikova M, Wania F, Donaldson DJ (2004) Atmos Environ 38:213–225, and references therein
60. Smyth CP (1955) Dielectric Behaviour and Structure. McGraw-Hill, New York
61. Velders GJM, Gillet JM, Becker PJ, Feil D (1991) J Phys Chem 95:8601–8608
62. McKinney JD (1989) Environ Health Perspect 82:323–336
63. Fraschini E, Bonati L, Pitea D (1996) J Phys Chem 100:10564–10569
64. Hirokawa S, Imasaka T, Imasaka T (2005) Chem Res Toxicol 18:232–238
65. Librando V, Alparone A (2007) Environ Sci Technol 41:1646–1652
66. Librando V, Alparone A (2007) Polycyclic Aromat Compd 27:65–94
67. Karelson M, Lobanov VS, Katritzky AR (1996) Chem Rev 96:1027–1044, and references therein
68. Singer KD, Garito AF (1981) J Chem Phys 75:3572–3580
69. Janssen RHC, Theodorou DN, Raptis S, Papadopoulos MG (1999) J Chem Phys 111:9711–9719
70. Chattaraj PK, Sengupta S (1996) J Phys Chem 100:16126–16130
71. Minisini B, Fayet G, Tsobnang F, Bardeau JF (2007) J Mol Model 13:1227–1235
72. Yu S, Herreno-Saenz D, Miller DW, Heflich RH, Kadlubar FF, Fu PP (1992) Mutat Res 283:45–52
73. Librando V, Alparone A (in press) J Hazard Mater , DOI 1016/j.jhazmat.20020